JBC RESEARCH ARTICLE

Cholinergic signaling at the body wall neuromuscular junction distally inhibits feeding behavior in *Caenorhabditis elegans*

Received for publication, February 12, 2021, and in revised form, November 13, 2021 Published, Papers in Press, December 3, 2021,
https://doi.org/10.1016/j.jbc.2021.101466

Patricia G. Izquierdo[1,*], Fernando Calahorro[1], Thibana Thisainathan[1], James H. Atkins[1], Johanna Haszczyn[1], Christian J. Lewis[1], John E. H. Tattersall[2], A. Christopher Green[2], Lindy Holden-Dye[1], and Vincent O'Connor[1]

From the [1]School of Biological Sciences, Faculty of Environmental and Life Sciences, University of Southampton, Southampton, United Kingdom; [2]Dstl, Defence Science and Technology Laboratory, Porton Down, Salisbury, Wiltshire, United Kingdom

Edited by Michael Shipston

Complex biological functions within organisms are frequently orchestrated by systemic communication between tissues. In the model organism *Caenorhabditis elegans*, the pharyngeal and body wall neuromuscular junctions are two discrete structures that control feeding and locomotion, respectively. Separate, the well-defined neuromuscular circuits control these distinct tissues. Nonetheless, the emergent behaviors, feeding and locomotion, are coordinated to guarantee the efficiency of food intake. Here, we show that pharmacological hyperactivation of cholinergic transmission at the body wall muscle reduces the rate of pumping behavior. This was evidenced by a systematic screening of the effect of the cholinesterase inhibitor aldicarb on the rate of pharyngeal pumping on food in mutant worms. The screening revealed that the key determinants of the inhibitory effect of aldicarb on pharyngeal pumping are located at the body wall neuromuscular junction. In fact, the selective stimulation of the body wall muscle receptors with the agonist levamisole inhibited pumping in a *lev-1*-dependent fashion. Interestingly, this response was independent of *unc-38*, an alpha subunit of the nicotinic receptor classically expressed with *lev-1* at the body wall muscle. This implies an uncharacterized *lev-1*-containing receptor underpins this effect. Overall, our results reveal that body wall cholinergic transmission not only controls locomotion but simultaneously inhibits feeding behavior.

The communication between tissues has an important role in physiological processes in health, disease, and stress conditions (1, 2). The communication between the skeletal muscle, liver, and adipose tissue during exercise is a clear example of tissue communication to control energy metabolism and insulin sensitivity in that particular stress condition (3). The imbalance of that communication causes an increase of energy expenditure associated with chronic disease or cachexia (4). This complex process is conserved from invertebrates to mammals and can be modeled in simpler organisms such as the fruit fly *Drosophila melanogaster* (5–7).

The survival of the model organism *Caenorhabditis elegans* depends on two essential behaviors, feeding and locomotion, as well as the ability to modify them according to the environmental cues. The external presence of bacteria, *C. elegans'* food, is a potent stimulus that modulates the rate of feeding by increasing the pharyngeal movements and the intake of bacteria (8–10). Interestingly, nematodes can modify their locomotory patterns according to food availability and changing between dwelling and roaming (11, 12). In this sense, the quality and quantity of food ingested emerges as an important environmental factor to modulate the worm's motility directly controlled by the neuromuscular body wall (12, 13). Similarly, mechanical stimulation or the optogenetic silencing of the body wall musculature reduces the feeding rate of *C. elegans* that is otherwise directly governed by cholinergic transmission at the pharyngeal neuromuscular junction (14–16). This supports the notion that locomotory function might provide additional pathways that contribute to regulation of the pharyngeal circuits that control feeding.

Morphologically, the pharynx is divided into three different parts: the corpus, the isthmus, and the terminal bulb. Two pharyngeal movements are responsible for the transport of bacteria by ingestion *via* the buccal cavity to the intestines (17–19). The coordinated contraction-relaxation cycle of the corpus and the terminal bulb causes the opening of the lumen in these parts of the pharynx that results in the aspiration of bacteria into the cavity. This rhythmic movement is named pharyngeal pumping and is caused by the release of acetylcholine and glutamate from the MC and M3 pharyngeal neurons that contract and relax the pharyngeal muscle, respectively (20, 21). The bacteria accumulated in the corpus during the pumping are directed to the terminal bulb by the progressive wavelike contractions of the muscles in the isthmus. This peristalsis movement depends on acetylcholine release from the pharyngeal motor neuron M4 (22, 23), one of the 20 neurons that more widely supports the regulation of feeding. This circuit is isolated from the rest of the animal by a basal lamina (17). A single synaptic connection is described between the pharynx and the rest of the animal (I2-RIP). However, disruption of this connection does not cause any

* For correspondence: Patricia G. Izquierdo, P.Gonzalez@soton.ac.uk.

defect in the feeding phenotype, indicating that this anatomical route does not mediate a strong determinant of the pharyngeal modulation of feeding (19). This points to a more important role of neuromodulatory signaling *via* biogenic amines and peptides, involving volume transmission (10).

In comparison to the body wall muscle, less is known about the molecular composition of the receptor organization that controls the pharyngeal neuromuscular junction and the feeding phenotype. The glutamate-gated chloride channel AVR-15 acts postsynaptically in the pharyngeal muscle to sense glutamate released from the motor neuron M3 that causes muscle relaxation (20, 24). EAT-2 is a cys-loop acetylcholine receptor subunit localized at the synapse between the pharyngeal MC motor neuron and the muscle at the corpus. It requires the auxiliary protein EAT-18 to allow EAT-2 essential function in initiating contraction (21, 25). Mutations in *avr-15* and *eat-2* phenocopy the feeding behavior of nematodes with M3 and MC ablated neurons respectively, highlighting the critical role these receptor components play (20, 21, 24). The feeding phenotype in addition requires the release of acetylcholine by the motor neuron M4, triggering isthmus peristalsis (23). However, there is not any mutation in an acetylcholine receptor that phenocopies the M4 ablation, and the molecular determinants of this feeding critical function are unknown.

To better define the molecular determinants of the pharyngeal neuromuscular junction of *C. elegans*, we performed a targeted screen of the pumping behavior on food with defined molecular determinants of cholinergic transmission in the presence or absence of aldicarb. This acetylcholinesterase inhibitor has been previously used to induce paralysis of movement, and this led to the discovery of molecular components at the body wall neuromuscular junctions in *C. elegans* (26, 27). We found that the genes conferring significant drug sensitivity of the pharyngeal paralysis are surprisingly located in the body wall neuromuscular junction. In addition, we describe how the stimulation of a LEV-1-containing receptor at the body wall reduced the pharyngeal pumping rate. This indicates an unexpected communication between the body wall neuromuscular junction that controls locomotion and the distinct and physically separated pharyngeal circuit that controls feeding.

Results

The determinants that control pharyngeal function are distinct from the determinants that control pharyngeal sensitivity to aldicarb

To investigate the cholinergic regulation and better describe the molecular determinants of the feeding behavior, the well-characterized protocol of aldicarb-induced paralysis was performed (26, 27). This assay has been extensively used to find molecular determinants at the neuromuscular junction of the body wall on the basis of resistance or hypersensitivity to paralysis of locomotion when nematodes are incubated on aldicarb-containing agar plates (26). We previously demonstrated that aldicarb and other cholinesterase inhibitors also cause a dose-dependent inhibition of the pharyngeal function (28). This inhibition was associated with the pharynx exhibiting hypercontraction observed by the opening of the lumen (28). This implied that aldicarb intoxication in the context of the whole organism would result from drug-induced hyperactivation of the cholinergic transmission. In this sense, we hypothesized that molecular determinants in the pharynx would confer resistance or hypersensitivity to aldicarb-induced paralysis of feeding behavior.

We screened the pharyngeal function of different mutant worms in the presence or absence of the cholinesterase-inhibitor aldicarb under the conditions we previously optimized (28). The results of this screening are listed in Table 1. It consisted of 56 mutant strains deficient in cholinergic and other neurotransmitter signaling. The components of the cholinergic pathway tested included alpha and non-alpha subunits of the acetylcholine-gated cation channel (29), subunits of the nematode-selective acetylcholine-gated chloride channel (30), muscarinic acetylcholine receptors (31–34), acetylcholinesterases (35–37), and auxiliary proteins involved in the proper function of the cholinergic receptors (21, 25, 38–47) (Table 1). We in addition included two nematode strains that exhibit hyperactivity at the body wall muscle (48, 49). In doing so, we have probed for molecules that represent structural or functional homologs of the receptors, trafficking or scaffolding molecules known to control archetypal cholinergic function and plasticity in higher animals (50). This analysis can be conveniently summarized by ascribing responses into three different groups of mutants regarding their pharyngeal pumping on food in the absence and presence of aldicarb (Fig. 1).

One class of mutants showed reduced pumping rate in the absence of aldicarb but WT inhibition of pharyngeal pumping in the presence of the drug (Fig. 1*A* and Table 1). This class of mutants clearly harbors an important contribution to feeding at physiological levels of cholinergic stimulation when nematodes are on food. However, despite this essential contribution, no resistance to the inhibition was observed when the cholinergic stimulation increased because of aldicarb exposure. According to this, we identified this class of mutants as "physiological determinants" of the feeding phenotype. This is exemplified by the *eat-2* and *eat-18* mutants. In addition, mutant nematodes deficient in the subunits of the acetylcholine-gated cation channel DEG-3, ACR-6, ACR-9, and ACR-10, the subunit of the acetylcholine-gated chloride channel ACC-3, and the calcineurin CNB-1 exhibited a similar pattern of reduced pumping when they are off drug and similar pharyngeal inhibition on aldicarb compared with the response shown by the N2 WT (Fig. 1*A*).

The second class of mutants essentially described the opposite of the above. These mutants showed normal pumping rate on food relative to N2 but clear resistance to the aldicarb-induced inhibition of the pharyngeal function observed in the WT treated worms (Fig. 1*B* and Table 1). The effect of this

Table 1
Pharyngeal pumping rate on food in the absence or presence of aldicarb

				Off aldicarb				On aldicarb				
Classification	Strain	Gene	Allele	Pumps/min ± SD	N	Stat	*p* value	Pumps/min ± SD	N	Stat	*p* value	% Inh
	N2			249.4 ± 12.1	52			9.5 ± 13.1	48			96.2
alpha-nAChR subunits	DH404	*unc-63*	*b404*	178.4 ± 20.6	12	****	<0.0001	47.1 ± 51.5	12	****	<0.0001	73.6
	VC1041	*lev-8*	*ok1519*	251 ± 9.8	6	ns	>0.9999	23.2 ± 26.7	5	ns	>0.9999	90.6
	ZZ20	*unc-38*	*x20*	230.8 ± 12.8	9	ns	>0.9999	22.8 ± 13.4	9	ns	>0.9999	90.1
	CB904	*unc-38*	*e264*	221 ± 15.9	12	*	0.0103	8 ± 7.9	12	ns	>0.9999	96.4
	TU1747	*deg-3*	*u662*	143.9 ± 65.9	8	****	<0.0001	7.1 ± 11.9	8	ns	>0.9999	95.1
	NC293	*acr-5*	*ok180*	253.8 ± 4.6	9	ns	>0.9999	4.3 ± 4.6	9	ns	>0.9999	98.3
	RB2294	*acr-6*	*ok3117*	185.1 ± 17.9	9	****	<0.0001	14.3 ± 27.1	9	ns	>0.9999	92.3
	FX863	*acr-7*	*tm863*	256.4 ± 5.6	9	ns	>0.9999	3.3 ± 5.1	9	ns	>0.9999	98.7
	RB1195	*acr-8*	*ok1240*	244.1 ± 7.2	9	ns	>0.9999	13.5 ± 11.6	9	ns	>0.9999	94.5
	RB2262	*acr-10*	*ok3064*	196.3 ± 49.9	6	****	<0.0001	2 ± 2.4	6	ns	>0.9999	99
	RB1263	*acr-11*	*ok1345*	252.6 ± 4.9	9	ns	>0.9999	3.1 ± 5.6	8	ns	>0.9999	98.8
	VC188	*acr-12*	*ok367*	252.6 ± 6.2	9	ns	>0.9999	76.8 ± 47.2	9	****	<0.0001	69.6
	RB1172	*acr-15*	*ok1214*	251.8 ± 2.2	7	ns	>0.9999	31.9 ± 24.2	7	ns	>0.9999	87.3
	RB918	*acr-16*	*ok789*	242.9 ± 3.4	9	ns	>0.9999	0.9 ± 1.4	9	ns	>0.9999	99.6
	RB1226	*acr-18*	*ok1285*	236.8 ± 10.5	9	ns	>0.9999	1.6 ± 1.6	9	ns	>0.9999	99.3
	DA1674	*acr-19*	*ad1674*	246.3 ± 8.6	8	ns	>0.9999	3.3 ± 2.5	8	ns	>0.9999	98.7
	RB1250	*acr-21*	*ok1314*	240 ± 9	8	ns	>0.9999	1.9 ± 2.2	8	ns	>0.9999	99.2
	RB2119	*acr-23*	*ok2804*	230.2 ± 5.9	9	ns	>0.9999	2.3 ± 2.2	9	ns	>0.9999	99
non-alpha nAChR subunits	CB193	*unc-29*	*e193*	227.3 ± 9.4	8	ns	0.749	52.3 ± 27	7	***	0.0005	77
	CB211	*lev-1*	*e211*	244.8 ± 10.6	15	ns	>0.9999	131.7 ± 61.1	15	****	<0.0001	46.2
	ZZ427	*lev-1*	*x427*	253.7 ± 17.8	4	ns	>0.9999	113.2 ± 72.5	4	****	<0.0001	55.4
	DA465	*eat-2*	*ad465*	50.3 ± 10.1	14	****	<0.0001	0.5 ± 0.6	11	ns	>0.9999	99
	RB1559	*acr-2*	*ok1887*	254.4 ± 5.7	8	ns	>0.9999	62.5 ± 59	8	****	<0.0001	75.4
	RB1659	*acr-3*	*ok2049*	235.8 ± 20.4	9	ns	>0.9999	21.8 ± 20.3	9	ns	>0.9999	90.8
	VC649	*acr-9*	*ok933*	217.3 ± 16.7	9	**	0.0040	11.3 ± 11	9	ns	>0.9999	94.8
	RB1132	*acr-14*	*ok1155*	250.8 ± 4.4	9	ns	>0.9999	0.8 ± 1.1	9	ns	>0.9999	99.7
	FX627	*acr-22*	*tm627*	227.1 ± 18.9	7	ns	>0.9999	5.9 ± 5.8	7	ns	>0.9999	97.4
	XA21193	*lev-1; unc-29*	*e211; e193*	250 ± 1.3	3	ns	>0.9999	115.1 ± 24.8	3	****	<0.0001	45
ACh-gated Cl channel subunits	VC1757	*acc-2*	*ok2216*	228.5 ± 28.4	9	ns	0.5222	20.5 ± 19.5	5	ns	>0.9999	90.3
	RB2490	*acc-3*	*ok3450*	153.7 ± 38.4	8	****	<0.0001	39.2 ± 37.7	7	ns	0.1027	74.5
	RB1832	*acc-4*	*ok2371*	225.3 ± 31.3	4	ns	>0.9999	5.5 ± 8.3	4	ns	>0.9999	97.6
mAChRs	RB896	*gar-1*	*ok755*	222.3 ± 7.5	4	ns	>0.9999	24.8 ± 47.5	4	ns	>0.9999	88.8
	RB756	*gar-2*	*ok520*	224.6 ± 11.3	6	ns	0.8023	12.5 ± 8.9	4	ns	>0.9999	94.4
	VC670	*gar-3*	*gk337*	252.8 ± 8.3	6	ns	>0.9999	7 ± 12.7	4	ns	>0.9999	97.2
AChEs	VC505	*ace-1*	*ok663*	226.3 ± 26.9	5	ns	>0.9999	2.8 ± 4.9	4	ns	>0.9999	98.8
	GG202	*ace-2*	*g72*	235.5 ± 4.8	3	ns	>0.9999	6.8 ± 6.3	3	ns	>0.9999	97.1
	PR1300	*ace-3*	*dc2*	235.6 ± 13.7	4	ns	>0.9999	3.6 ± 6.3	4	ns	>0.9999	98.5
Ancillary proteins	MF200	*ric-3*	*hm9*	201 ± 27.6	6	***	0.0001	74.1 ± 42	6	****	<0.0001	63.1
	CB306	*unc-50*	*e306*	223 ± 15	4	ns	>0.9999	8.7 ± 7.5	3	ns	>0.9999	96.1
	CB883	*unc-74*	*e883*	232.1 ± 4.3	4	ns	>0.9999	5.9 ± 7.4	4	ns	>0.9999	97.5
APs involved in location of nAChRs	RB1717	*lev-9*	*ok2166*	236.5 ± 14.8	6	ns	>0.9999	94.9 ± 66.5	4	****	<0.0001	59.9
	ZZ17	*lev-10*	*x17*	239.7 ± 8.6	6	ns	>0.9999	83.6 ± 49.9	4	****	<0.0001	65.1
	EN39	*oig-4*	*kr39*	227.4 ± 21.4	4	ns	>0.9999	7 ± 9.1	3	ns	>0.9999	97
	EN300	*rsu-1*	*kr300*	243.9 ± 9.9	4	ns	>0.9999	20.4 ± 36.8	4	ns	>0.9999	91.6
Other APs	DA1110	*eat-18*	*ad1110*	65.9 ± 8	6	****	<0.0001	1.6 ± 1.4	4	ns	>0.9999	97.6
	PR675	*tax-6*	*p675*	222.1 ± 15.6	4	ns	>0.9999	17.1 ± 14.9	4	ns	>0.9999	92.3
	KJ300	*cnb-1*	*jh103*	193.6 ± 15.4	6	****	<0.0001	1.8 ± 1.8	6	ns	>0.9999	99.1
	HK30	*unc-68*	*kh30*	231.2 ± 17.9	4	ns	>0.9999	21.3 ± 23.2	4	ns	>0.9999	90.8
	EN100	*molo-1*	*kr100*	249.4 ± 6.6	6	ns	>0.9999	19.4 ± 7.4	4	ns	>0.9999	92.2
BWM hyperactive signaling	QW37	*unc-2*	*zf35gf*	257.2 ± 3.9	6	ns	>0.9999	22.1 ± 6.9	6	ns	>0.9999	91.4
	IZ236	*Pmyo-3::unc-38(V/S), Pmyo-3::unc-29(L/S),* and *Pmyo-3::lev-1(L/S)*		246.9 ± 6.6	6	ns	>0.9999	10.5 ± 9.2	6	ns	>0.9999	95.7
NTs signaling	MT6308	*eat-4*	*ky5*	211.6 ± 13.9	4	ns	0.1148	9.6 ± 19.8	5	ns	>0.9999	95.5
	VC862	*cho-1*	*ok1069*	206 ± 38.7	4	*	0.023	29 ± 25.4	4	ns	>0.9999	85.9
	GR1321	*tph-1*	*mg280*	217.1 ± 12	4	ns	0.4609	13.3 ± 14.3	3	ns	>0.9999	93.9
	RB681	*cat-1*	*ok411*	241.5 ± 14.8	4	ns	>0.9999	30.5 ± 9.5	3	ns	>0.9999	87.4
	CB156	*unc-25*	*e156*	225 ± 5.1	4	ns	>0.9999	3.8 ± 4	4	ns	>0.9999	98.3

Synchronized L4 + 1 nematodes were incubated for 24 h on seeded plates containing aldicarb or vehicle control before pumps per minute was quantified. Percentage of inhibition (% inh) is indicated and was calculated as 1 – (pumps off aldicarb/pumps on aldicarb) * 100. Statistical analysis corresponds to the comparison between each strain and the N2 WT control in each condition (off and on aldicarb). The data are shown as mean ± SD. $^{ns}p \geq 0.05$; $^{*}p < 0.05$; $^{**}p < 0.01$; $^{***}p < 0.001$; $^{****}p < 0.0001$ by two-way ANOVA test followed by Bonferroni corrections.
Abbreviations: AChEs, acetylcholinesterases; APs, auxiliary proteins; mAChRs, muscarinic acetylcholine receptors; nAChR, acetylcholine-gated cation channel; ns, not significant; NTs, neurotransmitters.

second class of determinants in the pharyngeal function was only apparent when the cholinergic transmission was over-stimulated beyond the physiological levels by preventing acetylcholine degradation due to acetylcholinesterase inhibition by aldicarb. Therefore, we named this group "pharmacological determinants" of feeding. These mutants included the well-characterized subunits of the acetylcholine-gated cation channel UNC-29, ACR-2, ACR-12, and LEV-1, along with the auxiliary proteins LEV-9 and LEV-10 (Fig. 1*B*). Interestingly, all the pharmacological determinants of the pharyngeal function are essential determinants of the body wall neuromuscular transmission by either acting in the motor

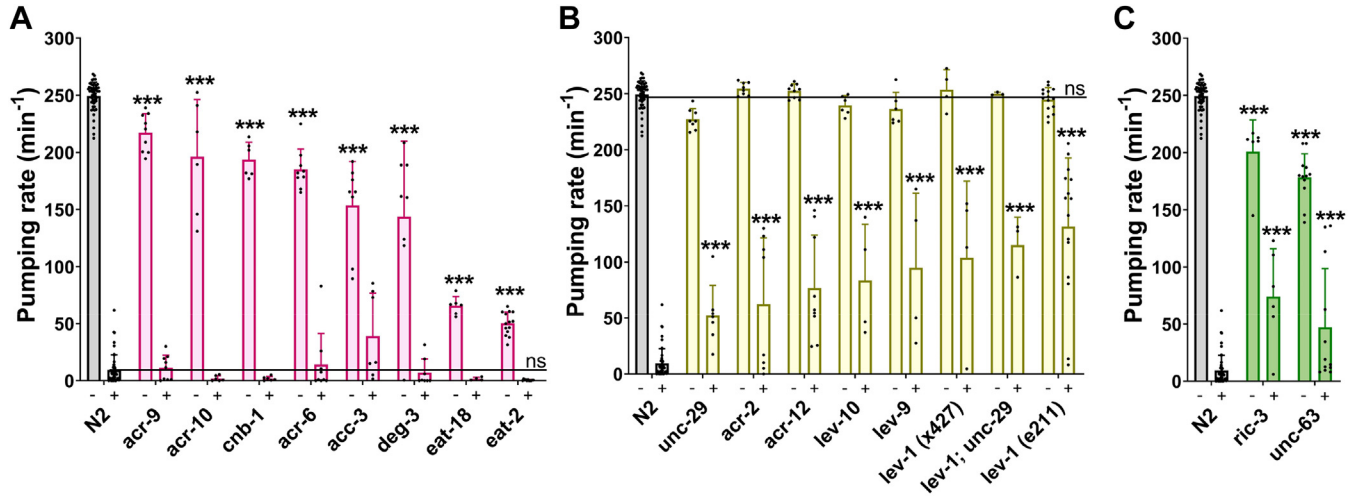

Figure 1. Molecular determinants that control pharyngeal function are distinct from the determinants that confer pharyngeal resistance to aldicarb. Pharyngeal pumping on food in the absence (–) or presence (+) of 500 μM aldicarb. *A*, mutant nematodes deficient in the non-alpha acetylcholine-gated cation channel subunits ACR-9 and EAT-2; the alpha acetylcholine-gated cation channel subunits ACR-10, ACR-6, and DEG-3; the acetylcholine-gated chloride channel subunit ACC-3; and the acetylcholine-receptor auxiliary proteins EAT-18 and CNB-1 exhibited a significant reduction of the pumping rate but a normal sensitivity to aldicarb compared with the WT control. *B*, mutant nematodes deficient in the non-alpha acetylcholine-gated cation channel subunits UNC-29, LEV-1, and ACR-2; the alpha acetylcholine-gated cation channel subunit ACR-12; and the acetylcholine-receptor auxiliary proteins LEV-9 and LEV-10 exhibited normal pumping rate on food but significant resistant to aldicarb compared with the WT worms. *C*, nematodes deficient in the ancillary protein RIC-3 and the alpha acetylcholine-gated cation channel subunit UNC-63 presented both phenotypes, reduced pumping rate on food, and resistance to aldicarb compared with the WT control. The data are shown as mean + SD of the pumping per minute. Statistical analysis corresponds to the same condition (absence or presence of aldicarb) between the N2 WT and each mutant strains. $^{ns}p > 0.05$; $^{***}p < 0.001$ by two-way ANOVA test. Refer to Table 1 for N numbers and *p* values.

neurons that release acetylcholine or postsynaptically in the body wall muscle (41, 42, 51, 52).

An important exception to this observation was the WT response to aldicarb of the *unc-38* alleles tested (Table 1). Despite their established role in body wall muscle sensitivity to acetylcholine and ensuing control of locomotion, these mutants expressed normal pumping on food and a WT sensitivity to aldicarb-induced inhibition of pharyngeal pumping.

To understand potential interaction between subunits that might define the aldicarb-induced inhibition of pharyngeal pumping on food, we compared the effect of aldicarb on the *lev-1*, *unc-29* single mutants and *lev-1; unc-29* double mutant. This comparison suggested no additive effect of combining the two mutations supporting the notion that they may act together in a single acetylcholine receptor. However, this is unlikely to be within the archetypal *unc-38* containing assemble that is classically studied at the body wall muscle of *C. elegans* (39).

Finally, the third class of mutants showed clear deficiency in the two distinct contexts, namely pumping on food in the absence of drug and resistance to aldicarb-induced inhibition of the pharyngeal function (Fig. 1*C* and Table 1). Only two mutants of the genes tested were encompassed in this group (Fig. 1*C*), the alpha subunit of the L-type receptor UNC-63 and the chaperone of the nicotinic receptors RIC-3 (53, 54).

Overall, the results suggest an unexpected divergence in cholinergic determinants of the pharyngeal function. Some of these control the physiological transmission that underpins fast pumping rate on food and others the hypothesized aldicarb-dependent process that executes an inhibition of feeding in the presence of the drug.

The pharyngeal function of C. elegans *exposed to levamisole exhibits a complex dose- and time-dependent inhibition*

The pharmacological determinants of the pharyngeal function highlighted in the previous screening with aldicarb (Fig. 1*B*) are known to underpin the mode of action of the nematode-selective pharmacological agent levamisole. This drug acts as an agonist of the body wall muscle nicotinic L-type receptor causing a spastic paralysis, essential for its use as a nematicide (55–57). Although distinct in its mode of action, levamisole, like aldicarb intoxication, leads to a hyperstimulation of the cholinergic synapses in the nematodes (57).

Accordingly, we investigated the levamisole response in the pharyngeal circuit to increasing concentrations of drug over the time by quantifying the pharyngeal pumping of WT worms (Fig. 2). Interestingly, the nematodes displayed a profound initial inhibition of pharyngeal pumping rate when placed on levamisole-containing plates (Fig. 2*A*). This reduction of the pharyngeal pumping was observed after control worms recovered from the mechanical stimulation caused by the picking process, which inhibits the feeding temporarily (Fig. 2*A*) (15). The IC_{50} value calculated after 10 min of incubation onto levamisole plates was 140 ± 1 μM (Fig. 2*B*).

After this initial inhibition of the pharyngeal function by levamisole, WT nematodes exhibited a partial recovery of the pumping rate over time at the lowest concentrations tested

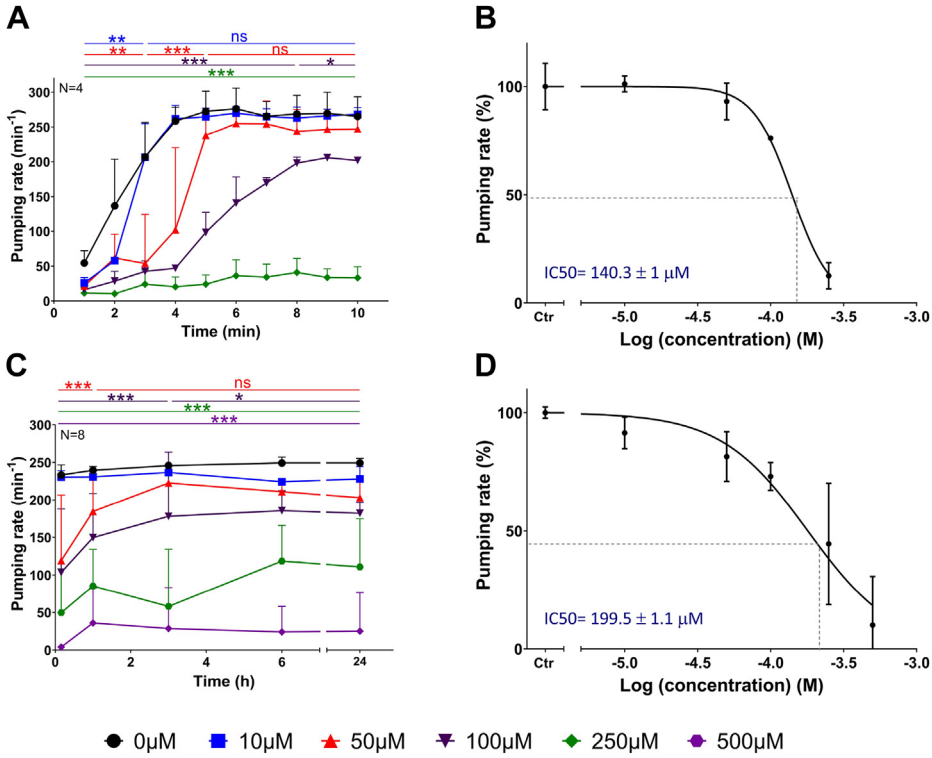

Figure 2. Pharyngeal function of *Caenorhabditis elegans* exposed to levamisole exhibited a complex concentration and time-dependent inhibition. *A*, pharyngeal pumping was quantified for synchronized L4 + 1 nematodes immediately after transferring to either naïve or levamisole-containing plates. The initial picking-mediated inhibition of pumping (15) was recovered within 4 min. The nematodes picked onto levamisole-containing plates displayed a delayed dose-dependent recovery of the pharyngeal function after picking. The data are shown as mean + SD of the pumping rate of four worms in four different experiments. *B*, IC50 value for pharyngeal inhibition by levamisole after 10 min of incubation. The curve corresponds to the following equation $y = 100/(1 + 10^{((-3.853 - x)*(-3.246))})$; $R^2 = 0.9663$; HillSlope = −3.246. *C*, pharyngeal pumping rate was quantified for synchronized L4 + 1 nematodes at different range of concentrations of levamisole over the time. An increased dose-dependent response was observed. The data are shown as mean ± SD of the pumping rate of eight worms in four different experiments per dose. *D*, IC50 value for pharyngeal inhibition by levamisole after 24 h of exposure. The curve corresponds to the following equation $y = 100/(1 + 10^{((-3.7 - x)*(-1.457))})$; $R^2 = 0.8080$; HillSlope = −1.457. Statistical analysis corresponds to the comparison between each concentration and the nondrug control in each end-point time of incubation. $^{ns}p > 0.05$; $*p < 0.05$; $**p < 0.01$; $***p < 0.001$ by two-way ANOVA test.

(10 µM and 50 µM), but the pumping was profoundly inhibited at the highest doses (250 µM and 500 µM) (Fig. 2*C*). This recovery of the pharyngeal function impacted on the IC_{50} value calculated, being 199 ± 1 µM after 24 h of incubation on levamisole-containing plates (Fig. 2*D*).

The fact that both levamisole and aldicarb inhibit pumping rate on WT worms and that *lev-1* deficient mutants are partially resistant to this effect for both drugs. This supports the hypothesis that the pharmacological hyperstimulation of the cholinergic system by either aldicarb or levamisole inhibits pharyngeal pumping by a common mechanism.

These data raised the idea that overactivity of the cholinergic system might act as the trigger to inhibit pharyngeal pumping. To assess this, we added genetic models that ape a hyperstimulated cholinergic transmission to our screen (QW37 and IZ236 strains in Table 1). We investigated the *unc-2 (zf35gf)* allele that has elevated acetylcholine release and the IZ236 strain engineered to overexpress a gain of function body wall muscle L-type receptor (48, 49). These strains showed no change in the expression of aldicarb-induced inhibition of pharyngeal pumping. Interestingly, despite harboring an intrinsically enhanced cholinergic tone, these strains did not have a *per se* change in their pharyngeal pumping. Thus, these genetic approaches do not mimic the signaling engaged by pharmacological activation *via* aldicarb.

The extra-pharyngeal nicotinic receptor subunit LEV-1 is a key determinant of levamisole inhibition of pharyngeal pumping

To more clearly resolve the molecular pathway through which the pharyngeal inhibition is mediated, we focused on the quantification of the pharyngeal function of *lev-1* deficient strains in the presence of levamisole (Fig. 3). The LEV-1 subunit was highlighted in our screen as the most significant determinant of the aldicarb-induced modulation of the feeding (Fig. 1*B*). In addition, the LEV-1 subunit was originally identified as a determinant of body wall muscle sensitivity to levamisole (51).

The strains deficient in *lev-1* displayed a similar inhibition of the pharyngeal function as WT worms after 10 min of incubation on 250 µM levamisole plates (Fig. 3). However, the pumping rate completely recovered over the time, being similar to the nondrug exposed nematodes after 3 h of incubation (Fig. 3, *B* and *C*). This phenotype was consistent in the two *lev-1* deficient strains tested, indicating the LEV-1 subunit of the nicotinic receptor is not responsible for the pharyngeal

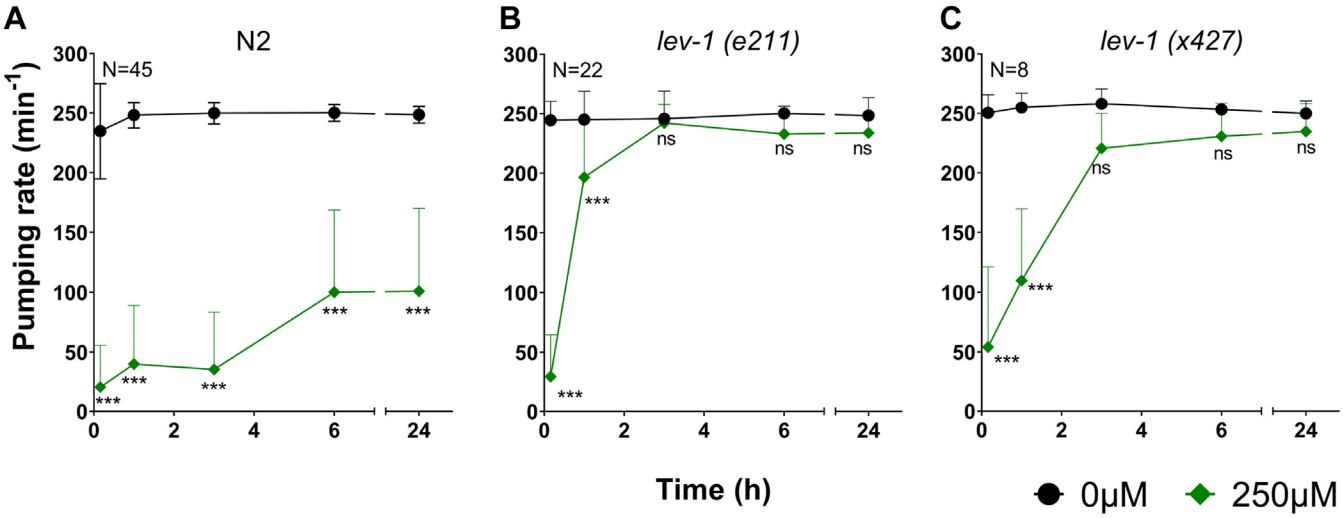

Figure 3. The non-alpha subunit LEV-1 of the heteromeric cholinergic receptor is responsible of the pharyngeal inhibition in the presence of levamisole at later end-point times. *A*, pharyngeal pumping was measured in the presence or absence of 250 µM of levamisole. The data are shown as mean ± SD of the pumping rate of 45 worms in at least 25 independent experiments. *B*, pumping rate of CB211 *lev-1* strain in the presence or absence of 250 µM levamisole. The data are shown as mean ± SD of 22 worms in at least ten independent experiments. *C*, pharyngeal pumping rate of ZZ427 *lev-1* mutant strain nematodes onto naïve or levamisole-containing plates. The data are shown as mean ± SD of the pumping per minute of eight nematodes in four independent experiments. Statistical analysis corresponds to the comparison between pumping rate on and off levamisole plates in each end-point time of incubation $^{ns}p > 0.05$; $^{***}p < 0.001$ by two-way ANOVA test.

inhibition by levamisole at early exposure times, but its function is indeed required at the later exposure times.

These results highlight two distinct components of a complex response to worm intoxication by levamisole. Although the rapid effect is independent of *lev-1*, the late sustained inhibition is clearly *lev-1* dependent. This points to an overlapping mechanism for the aldicarb- and levamisole-induced inhibition of the pharynx at protracted intoxication conditions. This mechanism is mediated by a LEV-1 containing receptor.

Because of the pivotal role played by LEV-1, we sought to detail its expression beyond the well characterized body wall muscle expression (51). We first investigated the expression of *lev-1* in the pharyngeal circuit of *C. elegans* using existing GFP translational reporters previously used to address functional expression of *lev-1* (58). Our analysis of these strains supported previous descriptions about the location in the body wall muscle cells as well as nerve ring, dorsal, and ventral nerve cord (Fig. 4*A*) (53, 58). However, the previous investigations highlighted that some pharyngeal gene expression can be masked by overlying nerve ring expression (59). To address this, pharynxes from transgenic worms carrying transcriptional (AQ585) and translational (AQ749) GFP reporters (58) were isolated and imaged to test for fluorescent signal (Fig. 4*A*). We did not observe GFP fluorescence in any of the isolated pharynx preparations, indicating the absence of LEV-1 expression in the isolated muscle or in its associated basal lamina embedded pharyngeal circuit (Fig. 4*A*).

This notion was reinforced using a different approach in which cDNA was synthesized from mRNA extracted from five pooled intact worms or five pooled isolated pharynxes. Specific amplification of *lev-1* was performed using SYBR Green. *myo-1* and *eat-2* were amplified in parallel as positive controls (Fig. 4*C*). We compared the relative abundance between the intact worm and isolated pharynxes by comparing the Ct values for each of these transcripts. This analysis showed robust amplification of the *lev-1* transcript from the cDNA from intact worms (Ct = 23; Fig. 4*C*), with two distinct pair of primers. In contrast, after 40 cycles, we failed to detect any amplification of *lev-1* using cDNA extracted from an equivalent number of isolated pharynxes (Ct = not-determined; Fig. 4*C*). This is consistent with *lev-1* expression falling below the limit of detection in a 40 cycles SYBR Green PCR. In contrast, two specific pharynx expressed transcripts, *myo-2* and *eat-2*, were equally amplified from both cDNAs, intact worms, and isolated pharynxes.

Taken together, these results indicate that the major pharmacological determinant of the drug-induced pharyngeal inhibition phenotype exerts its function outside the pharyngeal circuit.

LEV-1 is required in the body wall muscle to mediate levamisole inhibition of pharyngeal pumping

In view of the significance of LEV-1 in the body wall neuromuscular junction, we investigated tissue-specific rescue of LEV-1 at the musculature controlling the locomotion. For this, we generated transgenic lines of *lev-1* deficient nematodes expressing the WT cDNA version of the gene under the control of either *lev-1* or *myo-3* promoter. This experiment was replicated with two distinct *lev-1* deficient mutant strains (Fig. 5).

The naïve expression of *lev-1* rescued the WT pharyngeal sensitivity to levamisole in the two *lev-1* deficient mutants tested (Fig. 5). Furthermore, the phenotype was partially rescued in the *lev-1 (e211)* mutant strain (Fig. 5*A*) and fully rescued in the *lev-1 (x427)* mutant strain (Fig. 5*B*) when the WT version of the *lev-1* cDNA was selectively expressed in the body wall musculature under the control of the *myo-3* promoter.

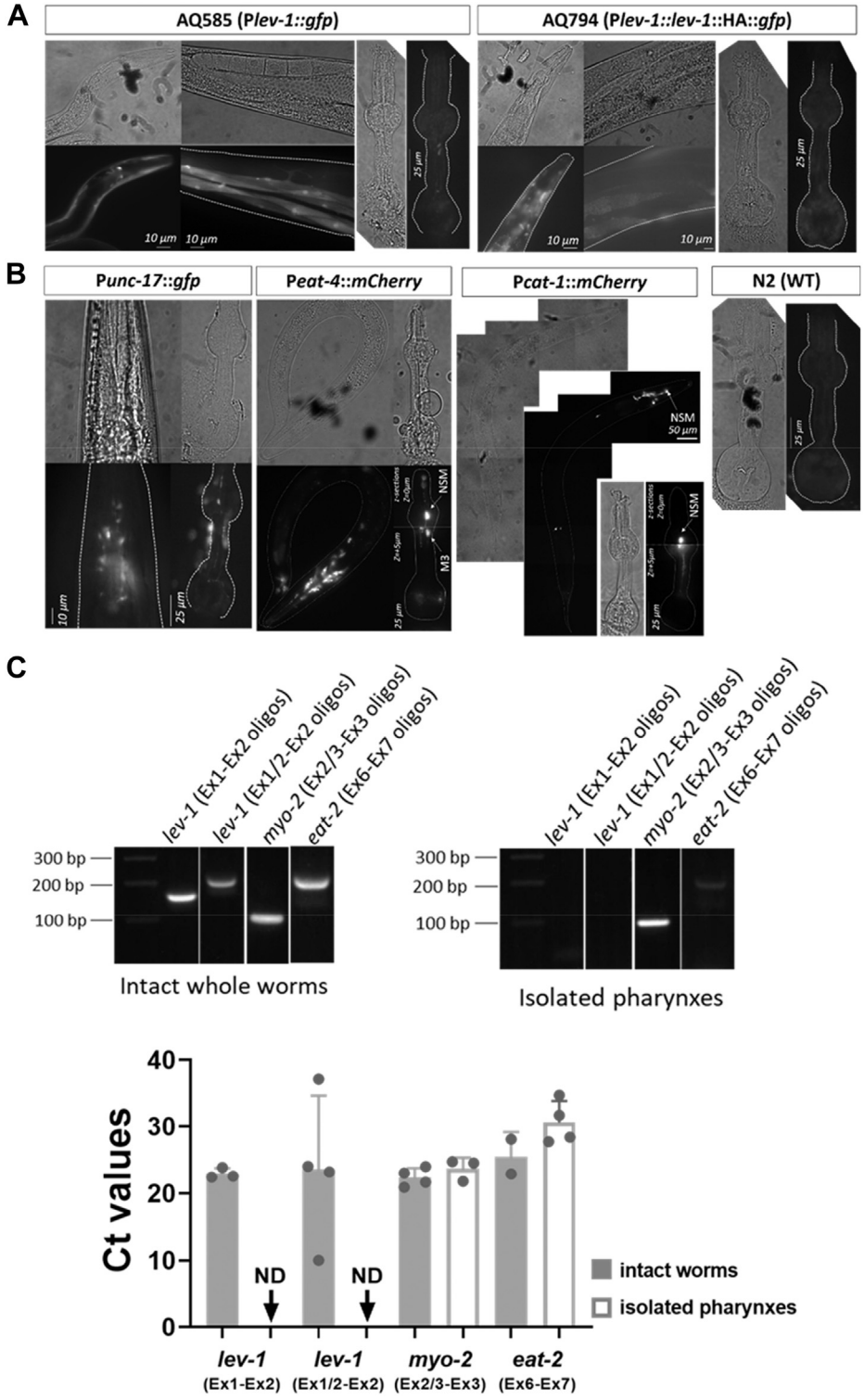

Figure 4. Differential dissection of isolated pharynx relative to intact worms does not detect expression of *lev-1* reporter constructs or *lev-1* transcripts in the pharynx. *A*, representative images of *lev-1* expression in both transcriptional and translational transgenic lines. The strain AQ585 corresponds to a transcriptional reporter expressing GFP under *lev-1* promoter in a WT background. The strain AQ749 corresponds to a translational reporter expressing the coding sequence of *lev-1* tagged with GFP under the control of *lev-1* naïve promoter in a *lev-1 (x427)* IV deficient background. *lev-1* is observed in body wall muscle and other head and body neurons in the intact worm. In micro dissected isolated pharynx, there is no detectable reported expression of *lev-1* (images to the *right* within each panel). *B*, representative images from isolated pharynxes derived from transgenic strains expressing fluorescence protein under the control of the cholinergic *unc-17* (GFP), glutamatergic *eat-4* (mCherry), or biogenic aminergic *cat-1* (mCherry) promoters. This shows the expected identity of distinct classes of pharyngeal neurons remain associated with the pharynx after micro-dissected isolation. The panel to the *right* shows the isolation of a pharynx from a N2 animal showing nonexpression. *C*, SYBR Green PCR of N2 WT isolated pharynxes demonstrates *lev-1* is not expressed of in the pharyngeal muscle or neuronal circuits. cDNA was reverse transcribed from RNA extracted from the pools of five single worms or five isolated pharynxes of WT nematodes. A comparative PCR was performed using primers for *lev-1* and two pharyngeal genes *myo-2* and *eat-2*. Representative amplification with the indicated primers is shown in the agarose gel images. The relative expression of these mRNAs was assessed based on

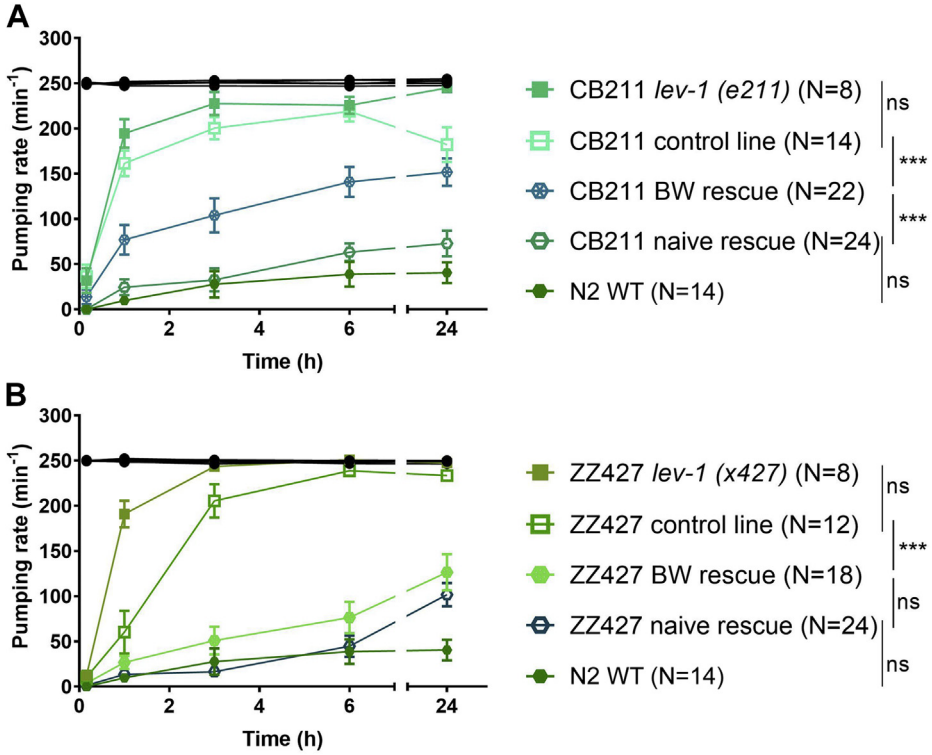

Figure 5. LEV-1 WT expression in body wall muscles of *lev-1* mutant nematodes restores the levamisole induced inhibition of the pharyngeal function. *A*, pharyngeal pumping in the absence (*black*) or presence (*green*) of 250 μM levamisole at different end-point times for N2, CB211 *lev-1 (e211)* mutant strain and transgenic lines expressing *lev-1* under either its own promoter (naïve rescue) or body wall muscle promoter (BW) into a CB211 background. The transgenic control lines were made by expressing GFP in coelomocytes of a *lev-1 (e211)*. The data are shown as mean ± SD of the pumping rate of 14 worms in at least seven different experiments for N2 WT, eight worms in at least five independent experiments for CB211 *lev-1 (e211)* mutant strain, 14 worms from two different lines in at least four independent experiments per line for control transgenic line, 22 worms from four different lines in at least three different experiments per line for body wall rescue transgenic lines, and 24 worms from four different lines in at least three different experiments per line for naïve rescue lines. *B*, pharyngeal pumping in the absence (*black*) or presence (*green*) of 250 μM levamisole at different end-point times for N2, ZZ427 *lev-1 (x427)* mutant strain and transgenic lines expressing *lev-1* under either its own promoter (naïve rescue) or body wall muscle promoter (BW) into a ZZ427 background. The transgenic control lines were made by expressing GFP in coelomocytes of a *lev-1 (x427)*. The data are shown as mean ± SD of the pumping rate of 14 worms in at least seven different experiments for N2 WT, eight worms in at least five independent experiments for ZZ427 *lev-1 (x427)* mutant strain, 12 worms from two different lines in at least three independent experiments per line for control transgenic line, 18 worms from three different lines in at least three different experiments per line for body wall rescue transgenic lines, and 24 worms from four different lines in at least three different experiments per line for naïve rescue lines. $^{ns}p > 0.05$; $^{***}p < 0.001$ by two-way ANOVA test.

These results indicate that the inhibition of the pharyngeal function by levamisole exposure is driven by the LEV-1 dependent signaling at the body wall muscle.

Neurohumoral signaling in C. elegans *has limited contribution to the pharyngeal sensitivity to levamisole*

Pharyngeal pumping rate in mutants deficient in major transmitters was investigated after 6 h of incubation with levamisole (Fig. 6), a time at which the inhibition of pumping rate by this drug was dependent on the LEV-1 function at the body wall neuromuscular junction (Figs. 3 and 5). These strains included those deficient in *unc-25 (e156)*, *eat-4 (ky5)*, *cat-1 (ok411)*, *tph-1 (mg280)*, *tdc-1 (n3419)*, *tbh-1 (n3247)*, and *egl-3 (n150)* (Fig. S1).

Nematodes deficient in the neurotransmitters GABA (*unc-25*), glutamate (*eat-4*), the biogenic amines (*cat-1*), serotonin (*tph-1*), octopamine (*tbh-1*), or both tyramine and octopamine (*tdc-1*), exhibited a similar response to levamisole compared with the WT nematodes. None of the mutant strains tested phenocopy the response observed in *lev-1* deficient worms, indicating limited contribution of these major transmitter pathways to the levamisole-induced inhibition of the pharyngeal circuit or the underlying pharyngeal muscle pumping. (Fig. 6).

Discussion

The screening performed in the present study was designed to identify molecular determinants that control the pharmacological inhibition of pumping during cholinergic hyperstimulation while comparing the cholinergic dependent intrinsic ability with respond to food (10). After this, we clearly defined three groups of determinants.

the Ct values in the reactions performed on intact worms and isolated pharynxes. This data shows that the robust detection of *lev-1* transcripts in whole worm cDNAs fell below the limits of detection (ND: not determined after saturating 40 cycles) from isolated pharynxes. In contrast, the amplification and transcript abundance were very similar in cDNA from intact worms and isolated pharynx tested for pharyngeal selective genes *eat-2* and *myo-2*. The data are shown as mean + SD.

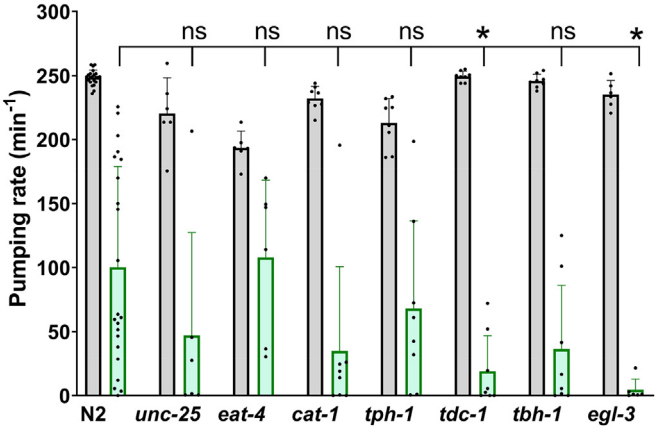

Figure 6. The inhibitory effect of levamisole on the pharyngeal function is independent of distinct classes of neurotransmitter, neurohumoral, and neuropeptidergic signaling. The pumping rate of indicated neuromodulatory deficient mutants on food in the absence (*gray column*) or presence (*green column*) of 250 μM of levamisole after 6 h incubation. See Fig. S1 for a cartoon summarizing the neurochemical deficiencies in the analyzed mutant backgrounds. Statistical analysis corresponds to the comparison between pumping rate on levamisole for N2 WT and the different mutant strains. The data are shown as mean + SD. $^{ns}p > 0.05$; $^{*}p < 0.05$ by two-way ANOVA test.

Physiological determinants of pharyngeal function

Although the pharyngeal muscle has two important cholinergic inputs in MC and M4 controlling its core function, there are additional cholinergic neurons of unknown function (17). Our study highlights an important class of mutants, including *eat-2* and *eat-18* deficient worms, which are fundamental to sustain high pumping rate on food in physiological conditions (Fig. 1*A*). Indeed, our comparative approach strongly reinforces the critical role of the EAT-2/EAT-18-dependent receptor (21, 25). The subunits of the nicotinic receptor ACR-6, ACR-10, DEG-3, and ACR-9 (29), the acetylcholine-gated chloride channel subunit ACC-3 (30) and the calcineurin CNB-1 (38) are included in this group (Fig. 7). This may have a value in better understanding the additional roles of cholinergic signaling and associated receptors in feeding behavior. However, further investigations will be required to identify the molecular pathways in which the physiological determinants of the feeding phenotype exert their function.

Interestingly, none of the mutants included in this group displayed resistance to aldicarb-induced inhibition of the pharyngeal function (Fig. 1*A*). It indicates that the physiological determinants responsible for the essential control of the pharynx are quite distinct from those that drive the inhibition in the presence of aldicarb. Indeed, the distinct nature of mutants reinforces this proposition (Fig. 7).

Pharmacological determinants of pharyngeal function

In the present study, we have used the aldicarb-induced paralysis protocol (26, 27) to investigate determinants that regulate the pharyngeal pumping behavior. However, this has highlighted a distinct nonpharyngeal modulation of drug-induced feeding inhibition. These investigations have been built on our previous observations indicating that aldicarb and other anti-cholinesterases cause a profound inhibition of the pharyngeal pumping (28). It was underpinned by a spastic paralysis of the radial muscles in the pharynx evidenced by an overt opening of the lumen (28). The prediction of our initial investigations was explained by assuming that aldicarb-dependent inhibition of acetylcholinesterase leads to an excess of input to the pharyngeal muscle from the two cholinergic motor neurons, MC and M4 (18, 23, 60, 61). In contrast to this view, we demonstrated here that LEV-1 and other molecular components of the body wall neuromuscular junction are strong determinants of the aldicarb-induced inhibition of the pharyngeal function (Fig. 1*B*). This points to the pivotal role of body wall muscle receptor in controlling locomotion and pharyngeal pumping in conditions where the pharmacological stimulation of the cholinergic signal causes an excitation of the musculature beyond the physiological levels (Fig. 7). This is reinforced by two observations: the failure to detect the *lev-1* expression in the pharynx (Fig. 4) and the tissue-specific rescue experiments in the *lev-1* mutant backgrounds (Fig. 5). The introduction of the WT version of *lev-1* in the body wall muscle had a strong rescue effect of the levamisole-induced inhibition of pumping (Fig. 5). However, we note that *lev-1* is expressed more widely than body wall muscle. Therefore, the expression in the nerve cord and nerve ring could in addition contribute to the integrity of the response.

A surprising extension of our work is that the body wall muscle receptor that organizes this coupling is not the same receptor that is classically associated with body wall function. This idea of different subunits composition creating a receptor at the body wall muscle has been previously insinuated in *C. elegans* and other nematodes (29, 62–64). Our conclusion emerges from the observation that *unc-38* mutants have a WT response to aldicarb-induced inhibition of pharyngeal function. In contrast, our analysis does support a role for both *lev-1* and *unc-29*. It is important to note that these two subunits would need to coassemble with an alpha-like subunit to make the functional receptor but the nature of the fully assembled receptor that triggers the coupling to distal pharyngeal inhibition remains to be resolved.

Overall, these results suggest that hyperstimulation of LEV-1-containing receptor at the body wall muscle modulates pharyngeal function by inhibiting the pumping rate in that particular stress condition. Indeed, feeding can continue after the ablation of the pharyngeal neurons (9) but can be completely abolished by mechanical stimulation of the nematodes (15) or optical silencing of the body wall musculature (14). In the present study, we demonstrated that the pharmacological stimulation of the cholinergic signal at the body wall neuromuscular junction causes the reduction of the pharyngeal pumping (Fig. 7). This is a clear example of inter-tissue communication that is advantageous to the worm, allowing the coupling of two distinct functions. The mechanism underpinning the communication between the body wall and the pharyngeal neuromuscular junction is still unknown. Previously published observations highlighted the implication of dense core vesicle release and innexins as part of this

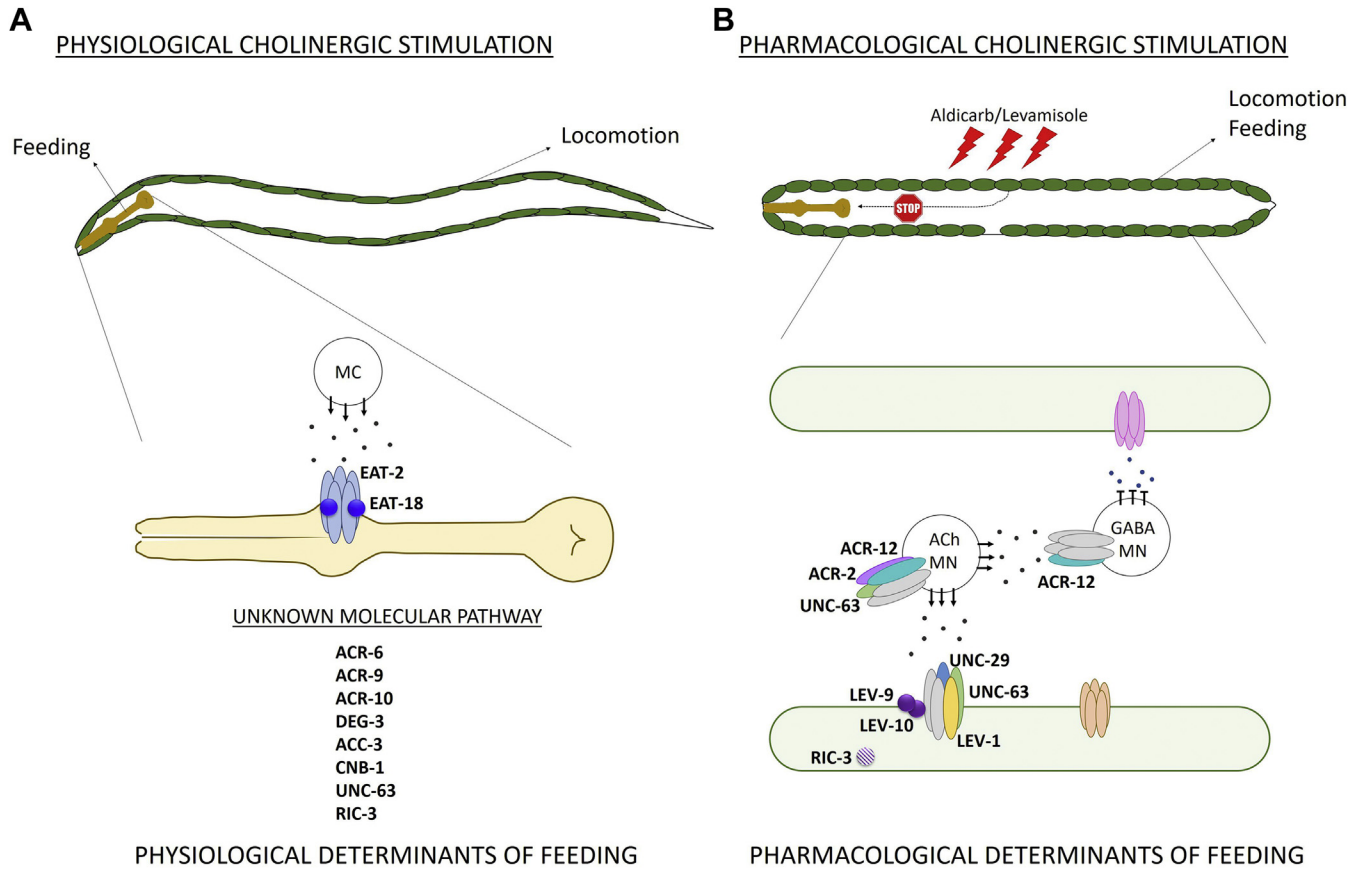

Figure 7. Physiological and pharmacological determinants of the feeding. The determinants of the pharyngeal function are distinct in the two contexts probed in this study. *A*, when nematodes are on food, the cholinergic transmission stimulates pumping that underpins physiological feeding. The determinants of the pumping rate are EAT-2 and EAT-18, transducing the MC cholinergic signal in the pharyngeal muscle (21, 25). The subunits of the nicotinic receptor ACR-6, ACR-9, ACR-10, DEG-3, ACC-3, UNC-63, the calcineurin subunit CNB-1, and the ancillary protein RIC-3 were identified as additional molecular determinants of pumping rate on food. *B*, the pharmacological overstimulation of the cholinergic pathway by aldicarb or levamisole drives activation body wall muscle that imposes inhibition of the pumping rate. In this context, a *lev-1* and *unc-29* containing receptor in the body wall musculature is involved in this response. The evidence suggests the subunits of the acetylcholine-gated ion channel UNC-63, UNC-29, LEV-1, ACR-2, ACR-12 and their auxiliary proteins LEV-9, LEV-10, and RIC-3 are important in modulating the body wall muscle activity that couples an inhibition of pharyngeal function. Interestingly, there is no *unc-38* dependence to this response precluding the classic L-type receptor in mediating the distal inhibition of feeding.

mechanism (14). Using our pharmacological paradigm, we did not identify clear routes of chemical transmission responsible for the coupling between feeding and locomotion (Figs. 6 and S1). Further investigations will be needed to underpin the signaling between the body wall and the pharyngeal circuits.

Determinants playing a role in both scenarios

A final class of mutants that emerged from the screen includes *unc-63* and *ric-3* deficient strains. These two mutants are the only ones tested that exhibited a deficit in the pumping rate on food in the absence of aldicarb and a resistance to the inhibition of pumping in the presence of the drug (Fig. 1*C*). Indeed, this facet of the response in the *unc-63* mutant indicates it is a candidate to coassemble with *lev-1* and possibly *unc-29* to generate the body wall receptor that couples to the inhibition of pharyngeal pumping. However, the fact that these mutants also impart the loss of the physiological pump rate on food suggests an under investigated role of UNC-63 and RIC-3 function within the pharyngeal circuit. This highlights paucity of understanding of the cholinergic determinants in pharyngeal function and how our screening approach may provide information about this in the future (Fig. 7).

Conclusion

In the *C. elegans* model organism, the ability of the pharynx to act as an interceptive cue for food to globally affect motility has been previously established (12). In the present work, we demonstrated that the pharmacological activation of the body wall circuit allows the distal inhibition of the pharyngeal pumping rate. This highlights a reverse route in which the tone of the musculature that controls locomotion impacts the circuit controlling the feeding behavior. This finding provides insight into how the functional state of one tissue can indirectly, but profoundly, impose control on distinct organs with an unrelated function. Acute regulation of pumping by the locomotory circuit has been noted (14, 15), however, the advantages and mechanisms for allowing this remain to be resolved. In a wider sense, this kind of inter-tissue communication can report stress or disease in the whole organism's physiology. In *C. elegans*, the hyperstimulation of the body wall

muscle might act as an aversive cue that impacts in the feeding rate of the worm. This presents similarities to the signals involved in disease in higher animals that impact on the appetite and feeding during cachexia (65).

Experimental procedures

C. elegans *maintenance and strains*

Nematodes were maintained at 20 °C on NGM plates supplemented with *Escherichia coli* OP50 strain as a source of food (66). The *C. elegans* mutant strains are listed in Table 1 and were provided by *Caenorhabditis* Genetics Center unless otherwise specified. The mutant strains EN39 *oig-4 (kr39)* II, EN300 *rsu-1 (kr300)* III, and EN100 *molo-1 (kr100)* III were kindly provided by Jean-Louis Bessereau Lab (Institut NeuroMyoGène). ZZ427 *lev-1 (x427)* and transgenic lines AQ585 corresponding to N2; *Ex [Plev-1::gfp; rol-6]* genotype and AQ749 corresponding to ZZ427 *lev-1 (x427)* IV; and *Is[Plev-1::lev-1::HA::gfp; rol-6]* genotype were kindly provided by William Schafer Lab (MRC Laboratory of Molecular Biology). QW37 *unc-2 (zf35gf)*X was kindly provided by Alkema Lab (UMass Chan Medical School). The transgenic line IZ236 *ufIs6 [Pmyo-3:: unc-38(V/S), Pmyo-3::unc-29(L/S), Pmyo-3:: lev-1(L/S)]* was kindly provided by Francis Lab (UMass Chan Medical School). The transgenic lines GE24 *pha-1 (e2123)* III; *Ex[Punc-17::gfp; pha-1 (+)]*, OH9279 otIs266 *(Pcat-1::mCherry)*, and N2; *Is[Peat-4::ChR2::mCherry]* were previously available in the laboratory stock. The double mutant strain XA211193 *lev-1 (e211)* IV; *unc-29 (e193)* I was generated in this work.

The following transgenic lines were generated in this work: VLP1: CB211 *lev-1 (e211)* IV; *Ex[Punc-122::gfp]*; VLP2: CB211 *lev-1 (e211)* IV; *Ex[Punc-122::gfp; Pmyo-3::lev-1]*; VLP3: ZZ427 *lev-1 (x427)* IV; *Ex[Punc-122::gfp]*; VLP4: ZZ427 *lev-1 (x427)* IV; *Ex[Punc-122::gfp; Pmyo-3::lev-1]*; VLP5: CB211 *lev-1 (e211)* IV; *Ex[Punc-122::gfp; Plev-1::lev-1]*; VLP6: ZZ427 *lev-1 (x427)* IV; and *Ex[Punc-122::gfp; Plev-1:lev-1]*.

Generation of lev-1 (e211) *and* unc-29 (e193) *double mutant*

lev-1; unc-29 double mutant strain (XA21193) was generated using previously described methods (67). Briefly, *lev-1 (e211)* males were induced by heat shock. Several young *lev-1 (e211)* males were incubated with three *unc-29 (e193)* hermaphrodites onto freshly seeded PO50 plates for 3 days. The mating was considered successful if the same rate of males and hermaphrodites was observed in the F1 generation. In this case, F1 hermaphrodites were heterozygous for both mutations lev-1 *(e211)* and *unc-29 (e193)*. Three F1 hermaphrodites were picked to individual plates and incubated till self-fertilization and egg-laying of the F2 generation. According to Mendel's laws, 1/16 of the F2 progeny would be homozygous for both mutations, *lev-1* and *unc-29*.

40 F2 hermaphrodites were incubated onto individual seeded plates to lay progeny (F3) and then picked into 2 µl of worm lysis buffer (5 mM Tris pH8, 0.25 mM EDTA, 0.5% Triton X100, 0.5% Tween 20, and 1 mg/ml proteinase K) into PCR tubes for genotyping. After spinning the tubes, the mixture was incubated at 65 °C for 10 min and at 85 °C for 1 min using a T100 thermocycler (Bio-Rad). 1 µl of the lysate was used to amplify *e211* mutation of *lev-1* (Fw_*lev-1*_I6: 5′- TGAAATAGAAAACGTGGGGG -3′ and Rv_*lev-1*_UTR: 5′- AAGTTGAAAATGAAAGAATAATGG -3′) and the *e193* mutation of *unc-29* (Fw_*unc-29*_E7: 5′- GGTATTTGGAAG TTGGACTGTG -3′ and Rv_*unc-29*_E10: 5′- GCTCAGATG CCGATTTTGGG -3′). PCR was performed using Phusion High-Fidelity PCR Master Mix with HF Buffer (Thermo Fisher Scientific) following manufacturer instructions. The fragments were analyzed by Sanger sequencing.

Generation of lev-1 *rescue constructs*

PCR amplifications were performed using Phusion High-Fidelity PCR Master Mix with HF Buffer (Thermo Fisher Scientific) following manufacturer instructions unless otherwise is specified.

PCR was used to amplify sequence for the *myo-3* promoter. 2.3 kb upstream of *myo-3* was amplified using the primers 5′ TCCTCTAGATGGATCTAGTGGTCGTGG 3′ and 5′ ACC AAGCTTGGGCTGCAGGTCGGCT 3′ (58 °C annealing temperature). This was subsequently cloned into pWormgate expression vector using the indicated restriction sites incorporated into the 5′ end of the oligonucleotides indicated above (HindIII/XbaI).

The primers 5′ ATGCTAGCTCTCATAACACTCAAG AAAACCCA 3′ and 5′ CCTCTATCCTCCACCACCTCCT AAC 3′ were used to amplify 3.536 kb of *lev-1 locus* corresponding to 3.5 kb upstream of the starting codon and 36 pb of exon one. PCR conditions for amplification were as follows: initial 3 min at 98 °C after 34 cycles consisting of 1 min at 98 °C, annealing 1 min at 57 °C, extension 3:30 min at 72 °C, and a final extension 10 min at 72 °C. The amplification product was cloned into pWormgate expression vector using the restriction site NheI underlined in forward primer and the naturally occurred XbaI restriction site 4 pb upstream of the *lev-1* starting codon.

cDNA of *lev-1* was amplified from a *C. elegans* cDNA library (OriGene) using 5′ AGAGAGAATGATGTTAGGAGG 3′ and 5′ AGTTGAAAATGAAAGAATAATGG 3′ (55 °C annealing temperature) forward and reverse primers, respectively. The PCR product was subcloned into pCR8/GW/TOPO following manufacturer protocol and subsequently cloned into pWormgate plasmid containing either *Pmyo-3* or *Plev-1* to generate *Pmyo-3::lev-1* and *Plev-1::lev-1* plasmids, respectively. The sequence of the plasmids was validated by Sanger sequencing before microinjection.

Generation of transgenic lines

The marker plasmid *Punc-122::gfp* was kindly provided by Antonio Miranda Lab (Instituto de Biomedicina de Sevilla). It drives the expression of GFP specifically in coelomocytes of *C. elegans* (68).

The microinjection procedure was performed as previously described (69). A concentration of 50 ng/µl of the marker plasmid *Punc-122::gfp* was injected into 1 day old adults of the

CB211 *lev-1 (e211)* IV and ZZ427 *lev-1 (x427)* IV mutant background to generate the transgenic strains VLP1 and VLP3, respectively. A mixture of 50 ng/μl of *Punc-122::gfp* plasmid and 50 ng/μl of *Pmyo-3::lev-1* plasmid was microinjected into the adults of CB211 and ZZ427 strains to produce the transgenic lines VLP2 and VLP4, respectively. Finally, the transgenic strains VLP5 and VLP6 were generated by microinjecting adults of the *lev-1 (e211)* and *lev-1 (x427)* mutant backgrounds, respectively, with a mixture of 50 ng/μl of *Punc-122::gfp* plasmid and 50 ng/μl of *Plev-1::lev-1* plasmid.

The genotype of CB211 and ZZ427 strains was authenticated by PCR amplification of the *lev-1* gene, and subsequent sequencing of the PCR product before microinjection was carried out.

Quantification of body wall and pharyngeal transcripts in both intact animals and isolated pharynxes

Five intact L4 + 1 worms or five isolated pharynxes were placed into 1 μl worm lysis buffer containing a final concentration of 5 mM Tris pH8, 0.25 mM EDTA, 0.5% Triton X100, 0.5% Tween 20, and 1 mg/ml proteinase K. After centrifugation for 5 s, the mixture containing either the intact worms or the isolated pharynxes was incubated at 65 °C for 10 min and at 85 °C for 1 min using a T100 thermocycler (Bio-Rad). The heated lysate was subsequently used in cDNA synthesis with SuperScript III Reverse Transcriptase kit in a total volume of 20 μl following manufacturer protocol (Invitrogen). 5 μl of the resulting cDNAs was used in PCR reactions using iQ SYBR Green Supermix and the indicated oligo primers. Each reaction contained 250 nM forward/reverse oligo primers and 10 μl iQ SYBR Green Supermix (final volume of 20 μl). Amplifications were performed in a 3-step real-time PCR protocol following recommendations for iQ SYBR Green Supermix: one cycle of initial denaturation and enzyme activation step at 95 °C for 3 min; after 40 cycles of denaturing at 95 °C for 15 s, annealing for 30 s, and extension at 72 °C for 30 s; finally, one cycle of melt curve 55 to 95 °C (in 0.5 °C increments) for 15 s. After completion of the 40 cycles reaction, the amplified products were resolved in a 2% agarose gel. The Ct values obtained for each reaction were used as a proxy for transcript abundance based on a normalization that each reaction had a fix number of worms or isolated pharynxes. At least two independent mRNA isolations and SYBR Green PCR were performed on independent days.

The primers used for the SYBR Green based PCRs were: 5′ GGACAGGGAGCCGAGAAGAC 3′ and 5′ GAAGCATC GTTAAGGAAAGTCAGG 3′ (64 °C annealing temperature, amplifying 109 bp) for *myo-2* (Ex2/3-Ex3); 5′ GTGAATAG TCAGTTGGTGATGG 3′ and 5′ TGCGAAAATAAGT GCTGTGGTG 3′ (66 °C annealing temperature, amplifying 207 bp) for *eat-2* (Ex6-Ex7); 5′ ATGTTAGGAGGTGGTGGA GG 3′ and 5′ GTTGAACGAGAGAGTTGTATCC 3′ (66 °C annealing temperature, amplifying 162 bp) for *lev-1* (Ex1-Ex2); and 5′- GTGTTTTTGGCAGTATCCCTCC -3 and 5′- TCCC ATTTCATAGTCAACCACAC -3′ (63 °C annealing temperature, amplifying 217 bp) for *lev-1* (Ex1/2-Ex2).

Plate husbandry

Aldicarb and levamisole hydrochloride (Merck) were dissolved in 70% ethanol and water, respectively. The stock drugs were kept at 4 °C and used within a month or discarded.

Behavioral experiments were performed at room temperature (20 °C) in 6-well plates that were prepared the day before each experiment. Drug-containing plates were made by adding a 1:1000 aliquot of the concentrated stock to molten tempered NGM agar to give the indicated concentrations of aldicarb (500 μM) and levamisole (10 μM–500 μM). For aldicarb control plates, a similar aliquot of 70% ethanol was added to the molten agar. The final concentration of ethanol for control and aldicarb-containing plates was 0.07%. This concentration of ethanol did not affect any of the behavioral tests performed in this work (data not shown).

For protracted intoxication experiments, 50 μl of OP50 bacteria culture at one A_{600} was pipetted onto the solidified NGM assay plates containing either drug or vehicle. For the first 10 min of exposure to levamisole (early intoxication experiment), assay plates were seeded with 100 μl of OP50 bacteria culture of one A_{600} that was spread evenly over the complete surface of the NGM agar. After seeding, plates were left in the laminar flow hood for 1 h to facilitate drying of the bacterial lawn. 6-well plates containing either levamisole or aldicarb with bacterial lawn were then stored in dark at 4 °C until next day. Assay plates were incubated at room temperature for at least 30 min before starting the experiment. Contrary to assay plates with other cholinergic drugs (70), we did not observe any difference in the density or integrity of the bacterial lawn between control and drugged plates.

Behavioral observations

A pharyngeal pump cycle consists of contraction-relaxation of the terminal bulb in the pharyngeal muscle. Each pump was discerned by the backward-forward movement of the grinder structure in the terminal bulb. The pharynx was observed using a Nikon SMZ800 (×60 magnification) binocular dissecting microscope. The movement of the grinder within terminal bulb of the pharynx was counted by visually registering on a hand-held clicker counting. Each grinder movement was recorded as a single pump and the number of pumps measured for 1 min.

For protracted intoxication experiments, the synchronized nematodes 1 day older than L4 stage (L4 + 1) were transferred onto the assay plates and the pumping measured after 24 h for aldicarb-intoxication assays and after 10 min, 1, 3, 6, and 24 h for levamisole-intoxication experiments. The nematodes that left the patch of food during the experiment were picked back to the bacterial lawn, and the pumping rate was scored after waiting 10 to 15 min.

For the first 10 min of exposure to levamisole, the synchronized (L4 + 1) adults were picked onto either control or levamisole-containing plates. The delay between each pump was scored for the consecutive 10 min straight after transferring each worm using Countdown Timer tool from www.WormWeb.org website. It was then translated into pumping rate per second.

The percentage of pharyngeal-pumping inhibition relative to the control after either 10 min or 24 h of incubation with levamisole was used to estimate IC_{50} values. The dose-curves were fitted according to the formula log (concentration) *versus* % maximum pump response measured in the absence of drug. The equation and parameters of each curve is specified in each figure legend.

Pharynx dissection procedure

Pharynxes were dissected according to previously published methods (71). Young adult (L4 + 1) worms were placed into dissection plates containing 3 ml of Dent's solution (glucose 10 mM, Hepes 10 mM, NaCl 140 mM, KCl 6 mM, $CaCl_2$ 3 mM, $MgCl_2$ 1 mM; pH 7.4) supplemented with 0.2% bovine serum albumin (Merck) (72). The dishes were incubated at 4 °C for 5 min to reduce the thrashing activity of the nematodes and then placed under a binocular microscope Nikon SMZ800. The lips of the worms were dissected from the rest of the body by making an incision with a surgical scalpel blade. Because of the internal pressure of the inside organs of the worm, the content is ejected outside the cuticle of the nematode leaving the pharynx and its embedded neural circuit exposed. When the terminal bulb was clearly observed outside the cuticle, a second incision was made at the pharyngeal-intestinal valve to isolate the pharynx from the rest of the intestine (Fig. 4). The pharynxes lacking more than half of the procorpus after dissection were not considered for either imaging or for RT-PCR.

Differential interference contrast and fluorescence imaging of pharyngeal structure and transgene expression

The isolated pharynxes were removed from the dissection dishes using nonsticky tips within 10 µl of solution. Fat and debris were carefully removed from the pharynxes by two sequential transfers, in a volume of 10 µl, through two changes of 3 ml Dent's 0.2% bovine serum albumin medium. After washing, the pharynxes were placed on a thin pad of 2% agarose previously deposited and solidified on a microscope slide. A 24 × 24 mm coverslip was gently located on top before observations were made. The objectives of 10×/0.30, 60× A/1.40 (oil), and 100× A/1.40 (oil) fitted in a Nikon Eclipse (E800) microscope were used to collect images through both differential interference contrast and epifluorescence filters. A Nikon C-SHG1 high pressure mercury lamp was used for illumination in fluorescence micrographs.

The images were acquired through a Hamamatsu Photonics camera software and were cropped to size, assembled, and processed using Abode PhotoShop (Adobe Systems) and ImageJ (NIH) software.

Three transgenic strains harboring *Punc-17::gfp*; *Peat-4::mCherry*; and *Pcat-1::mCherry* were used as control of the dissection procedure. These three strains are transcriptional reporters of cholinergic, glutamatergic, and monoaminergic neurons, respectively. The isolated pharynxes from the three transgenic strains were isolated and imaged after the previously explained protocol. Fluorescence from distinct neurons was observed upon the dissection procedure (Fig. 4*B*), indicating the pharyngeal neurons were preserved in the isolated pharynx preparations.

Statistical analysis

The collection of the data was performed blind, so the experimenter was unaware of the genotype and the drug present, absent, or concentration tested in each trial.

The data were analyzed using GraphPad Prism 8 and are displayed as mean ± SD. Statistical significance was assessed using two-way ANOVA after post hoc analysis with Bonferroni corrections where applicable. This post hoc test was selected among others to avoid false positives. The sample size N of each experiment is specified in the corresponding figure.

Data availability

All data presented are available upon request from Patricia G. Izquierdo (P.Gonzalez@soton.ac.uk).

Supporting information—This article contains supporting information.

Acknowledgments—We thank Dr Jean-Louis Bessereau, Dr Denise Walker, Dr William Schafer, Dr Mark Alkema, and Dr Michael Francis for sharing strains; and Dr Antonio Miranda-Vizuete for sharing *Punc-122::gfp* marker plasmid. We thank Emeritus Professor Robert Walker and Dr Helena Rawsthorne-Manning for critical reading of the article and for detailed comments.
Additional *C. elegans* strains were provided by the CGC, which is funded by NIH Office of Research Infrastructure Programs (P40 OD010440). This work was funded by the University of Southampton (United Kingdom) and the Defence Science and Technology Laboratory, Porton Down, Wiltshire (United Kingdom). The content is solely the responsibility of the authors and does not necessarily represent the official views of the National Institutes of Health.

Author contributions—P. G. I., J. E. H. T., A. C. G., L. H.-D., and V. O. conceptualization; P. G. I. data curation; P. G. I. and F. C. formal analysis; P. G. I., F. C., T. T., J. H. A., J. H., and C. J. L. investigation; P. G. I., F. C., J. E. H. T., A. C. G., L. H.-D., and V. O. methodology; P. G. I. validation; P. G. I. visualization; P. G. I. writing–original draft; P. G. I., F. C., J. E. H. T., A. C. G., L. H.-D., and V. O. writing–review and editing; J. E. H. T., A. C. G., L. H.-D., and V. O. funding acquisition; J. E. H. T., A. C. G., L. H.-D., and V. O. supervision.

Conflict of interest—The authors declare that they have no conflicts of interest with the contents of this article.

Abbreviations—The abbreviations used are: AChEs, acetylcholinesterases; APs, auxiliary proteins; mAChRs, muscarinic

acetylcholine receptors; nAChR, acetylcholine-gated cation channel; nd, not determined; ns, not significant; NTs, neurotransmitters.

References

1. Karsenty, G., and Olson, E. N. (2016) Bone and muscle endocrine functions: Unexpected paradigms of inter-organ communication. *Cell* **164**, 1248–1256
2. Rai, M., and Demontis, F. (2016) Systemic nutrient and stress signaling via myokines and myometabolites. *Annu. Rev. Physiol.* **78**, 85–107
3. Egan, B., and Zierath, J. R. (2013) Exercise metabolism and the molecular regulation of skeletal muscle adaptation. *Cell Metab.* **17**, 162–184
4. Argiles, J. M., Stemmler, B., Lopez-Soriano, F. J., and Busquets, S. (2018) Inter-tissue communication in cancer cachexia. *Nat. Rev. Endocrinol.* **15**, 9–20
5. Delanoue, R., Slaidina, M., and Leopold, P. (2010) The steroid hormone ecdysone controls systemic growth by repressing dMyc function in Drosophila fat cells. *Dev. Cell* **18**, 1012–1021
6. Demontis, F., and Perrimon, N. (2009) Integration of insulin receptor/Foxo signaling and dMyc activity during muscle growth regulates body size in Drosophila. *Development* **136**, 983–993
7. Rajan, A., and Perrimon, N. (2011) Drosophila as a model for interorgan communication: Lessons from studies on energy homeostasis. *Dev. Cell* **21**, 29–31
8. Avery, L., and Horvitz, H. R. (1990) Effects of starvation and neuroactive drugs on feeding in Caenorhabditis-elegans. *J. Exp. Zool.* **253**, 263–270
9. Avery, L., and Horvitz, R. (1989) Pharyngeal pumping continues after laser killing of the pharyngeal nervous-system of C-elegans. *Neuron* **3**, 473–485
10. Dalliere, N., Bhatla, N., Luedtke, Z., Ma, D. K., Woolman, J., Walker, R. J., Holden-Dye, L., and O'Connor, V. (2016) Multiple excitatory and inhibitory neural signals converge to fine-tune Caenorhabditis elegans feeding to food availability. *FASEB J.* **30**, 836–848
11. Sawin, E. R., Ranganathan, R., and Horvitz, H. R. (2000) C-elegans locomotory rate is modulated by the environment through a dopaminergic pathway and by experience through a serotonergic pathway. *Neuron* **26**, 619–631
12. Ben Arous, J., Laffont, S., and Chatenay, D. (2009) Molecular and sensory basis of a food related two-state behavior in C. elegans. *PLoS One* **4**, e7584
13. Shtonda, B. B., and Avery, L. (2006) Dietary choice behavior in Caenorhabditis elegans. *J. Exp. Biol.* **209**, 89–102
14. Takahashi, M., and Takagi, S. (2017) Optical silencing of body wall muscles induces pumping inhibition in Caenorhabditis elegans. *PLoS Genet.* **13**, e1007134
15. Chalfie, M., Sulston, J. E., White, J. G., Southgate, E., Thomson, J. N., and Brenner, S. (1985) The neural circuit for touch sensitivity in Caenorhabditis-elegans. *J. Neurosci.* **5**, 956–964
16. Keane, J., and Avery, L. (2003) Mechanosensory inputs influence Caenorhabditis elegans pharyngeal activity via ivermectin sensitivity genes. *Genetics* **164**, 153–162
17. Albertson, D. G., and Thomson, J. N. (1976) The pharynx of Caenorhabditis elegans. *Philos. Trans. R. Soc. Lond. B Biol. Sci.* **275**, 299–325
18. Avery, L. (1993) The genetics of feeding in *Caenorhabditis elegans*. *Genetics* **133**, 897–917
19. Avery, L., and Thomas, J. H. (1997) Chapter 24: Feeding and defecation. In: Riddle, D. L., Blumenthal, T., Meyer, B. J., Priess, J. R., eds. *C. elegans II*, Cold Spring Harbor Laboratory Press, Cold Spring Harbor, NY
20. Avery, L. (1993) Motor-neuron M3 controls pharyngeal muscle-relaxation timing in Caenorhabditis-elegans. *J. Exp. Biol.* **175**, 283–297
21. McKay, J. P., Raizen, D. M., Gottschalk, A., Schafer, W. R., and Avery, L. (2004) eat-2 and eat-18 are required for nicotinic neurotransmission in the Caenorhabditis elegans pharynx. *Genetics* **166**, 161–169
22. Avery, L., and Shtonda, B. B. (2003) Food transport in the C-elegans pharynx. *J. Exp. Biol.* **206**, 2441–2457
23. Avery, L., and Horvitz, H. R. (1987) A cell that dies during wild-type C-elegans development can function as a neuron in a Ced-3 mutant. *Cell* **51**, 1071–1078
24. Dent, J. A., Davis, M. W., and Avery, L. (1997) avr-15 encodes a chloride channel subunit that mediates inhibitory glutamatergic neurotransmission and ivermectin sensitivity in Caenorhabditis elegans. *EMBO J.* **16**, 5867–5879
25. Choudhary, S., Buxton, S. K., Puttachary, S., Verma, S., Mair, G. R., McCoy, C. J., Reaves, B. J., Wolstenholme, A. J., Martin, R. J., and Robertson, A. P. (2020) EAT-18 is an essential auxiliary protein interacting with the non-alpha nAChR subunit EAT-2 to form a functional receptor. *PLoS Pathog.* **16**, e1008396
26. Mahoney, T. R., Luo, S., and Nonet, M. L. (2006) Analysis of synaptic transmission in Caenorhabditis elegans using an aldicarb-sensitivity assay. *Nat. Protoc.* **1**, 1772–1777
27. Oh, K. H., and Kim, H. (2017) Aldicarb-induced paralysis assay to determine defects in synaptic transmission in Caenorhabditis elegans. *Bio Protoc.* **7**, e2400
28. Izquierdo, P. G., O'Connor, V., Green, A. C., Holden-Dye, L., and Tattersall, J. E. H. (2020) C. elegans pharyngeal pumping provides a whole organism bio-assay to investigate anti-cholinesterase intoxication and antidotes. *Neurotoxicology* **82**, 50–62
29. Holden-Dye, L., Joyner, M., O'Connor, V., and Walker, R. J. (2013) Nicotinic acetylcholine receptors: A comparison of the nAChRs of Caenorhabditis elegans and parasitic nematodes. *Parasitol. Int.* **62**, 606–615
30. Putrenko, I., Zakikhani, M., and Dent, J. A. (2005) A family of acetylcholine-gated chloride channel subunits in Caenorhabditis elegans. *J. Biol. Chem.* **280**, 6392–6398
31. Culotti, J. G., and Klein, W. L. (1983) Occurrence of muscarinic acetylcholine receptors in wild type and cholinergic mutants of Caenorhabditis elegans. *J. Neurosci.* **3**, 359–368
32. Hwang, J. M., Chang, D. J., Kim, U. S., Lee, Y. S., Park, Y. S., Kaang, B. K., and Cho, N. J. (1999) Cloning and functional characterization of a Caenorhabditis elegans muscarinic acetylcholine receptor. *Recept. Channels* **6**, 415–424
33. Lee, Y. S., Park, Y. S., Chang, D. J., Hwang, J. M., Min, C. K., Kaang, B. K., and Cho, N. J. (1999) Cloning and expression of a G protein-linked acetylcholine receptor from Caenorhabditis elegans. *J. Neurochem.* **72**, 58–65
34. Lee, Y. S., Park, Y. S., Nam, Y., Suh, S. J., Lee, F., Kaang, B. K., and Cho, N. J. (2000) Characterization of GAR-2, a novel G protein-linked acetylcholine receptor from Caenorhabditis elegans. *J. Neurochem.* **75**, 1800–1809
35. Combes, D., Fedon, Y., Grauso, M., Toutant, J. P., and Arpagaus, M. (2000) Four genes encode acetylcholinesterases in the nematodes Caenorhabditis elegans and Caenorhabditis briggsae. cDNA sequences, genomic structures, mutations and *in vivo* expression. *J. Mol. Biol.* **300**, 727–742
36. Selkirk, M. E., Lazari, O., Hussein, A. S., and Matthews, J. B. (2005) Nematode acetylcholinesterases are encoded by multiple genes and perform non-overlapping functions. *Chem. Biol. Interact.* **157**, 263–268
37. Selkirk, M. E., Lazari, O., and Matthews, J. B. (2005) Functional genomics of nematode acetylcholinesterases. *Parasitology* **131**, S3–S18
38. Bandyopadhyay, J., Lee, J., Lee, J., Lee, J. I., Yu, J. R., Jee, C., Cho, J. H., Jung, S., Lee, M. H., Zannoni, S., Singson, A., Kim, D. H., Koo, H. S., and Ahnn, J. (2002) Calcineurin, a calcium/calmodulin-dependent protein phosphatase, is involved in movement, fertility, egg laying, and growth in Caenorhabditis elegans. *Mol. Biol. Cell* **13**, 3281–3293
39. Boulin, T., Gielen, M., Richmond, J. E., Williams, D. C., Paoletti, P., and Bessereau, J. L. (2008) Eight genes are required for functional reconstitution of the Caenorhabditis elegans levamisole-sensitive acetylcholine receptor. *Proc. Natl. Acad. Sci. U. S. A.* **105**, 18590–18595
40. Boulin, T., Rapti, G., Briseno-Roa, L., Stigloher, C., Richmond, J. E., Paoletti, P., and Bessereau, J. L. (2012) Positive modulation of a Cys-loop acetylcholine receptor by an auxiliary transmembrane subunit. *Nat. Neurosci.* **15**, 1374–1381
41. Briseno-Roa, L., and Bessereau, J. L. (2014) Proteolytic processing of the extracellular scaffolding protein LEV-9 is required for clustering acetylcholine receptors. *J. Biol. Chem.* **289**, 10967–10974

42. Gally, C., Eimer, S., Richmond, J. E., and Bessereau, J. L. (2004) A transmembrane protein required for acetylcholine receptor clustering in Caenorhabditis elegans. *Nature* **431**, 578–582
43. Gendrel, M., Rapti, G., Richmond, J. E., and Bessereau, J. L. (2009) A secreted complement-control-related protein ensures acetylcholine receptor clustering. *Nature* **461**, 992–996
44. Gottschalk, A., Almedom, R. B., Schedletzky, T., Anderson, S. D., Yates, J. R., and Schafer, W. R. (2005) Identification and characterization of novel nicotinic receptor-associated proteins in Caenorhabditis elegans. *EMBO J.* **24**, 2566–2578
45. Maryon, E. B., Coronado, R., and Anderson, P. (1996) unc-68 encodes a ryanodine receptor involved in regulating C-elegans body-wall muscle contraction. *J. Cell Biol.* **134**, 885–893
46. Pierron, M., Pinan-Lucarre, B., and Bessereau, J. L. (2016) Preventing illegitimate extrasynaptic acetylcholine receptor clustering requires the RSU-1 protein. *J. Neurosci.* **36**, 6525–6537
47. Rapti, G., Richmond, J., and Bessereau, J. L. (2011) A single immunoglobulin-domain protein required for clustering acetylcholine receptors in C. elegans. *EMBO J.* **30**, 706–718
48. Huang, Y. C., Pirri, J. K., Rayes, D., Gao, S., Mulcahy, B., Grant, J., Saheki, Y., Francis, M. M., Zhen, M., and Alkema, M. J. (2019) Gain-of-function mutations in the UNC-2/CaV2alpha channel lead to excitation-dominant synaptic transmission in Caenorhabditis elegans. *Elife* **8**, e45905
49. Bhattacharya, R., Touroutine, D., Barbagallo, B., Climer, J., Lambert, C. M., Clark, C. M., Alkema, M. J., and Francis, M. M. (2014) A conserved dopamine-cholecystokinin signaling pathway shapes context-dependent Caenorhabditis elegans behavior. *PLoS Genet.* **10**, e1004584
50. Treinin, M., and Jin, Y. (2021) Cholinergic transmission in C. elegans: Functions, diversity, and maturation of ACh-activated ion channels. *J. Neurochem.* **158**, 1274–1291
51. Fleming, J. T., Squire, M. D., Barnes, T. M., Tornoe, C., Matsuda, K., Ahnn, J., Fire, A., Sulston, J. E., Barnard, E. A., Sattelle, D. B., and Lewis, J. A. (1997) Caenorhabditis elegans levamisole resistance genes lev-1, unc-29, and unc-38 encode functional nicotinic acetylcholine receptor subunits. *J. Neurosci.* **17**, 5843–5857
52. Jospin, M., Qi, Y. B., Stawicki, T. M., Boulin, T., Schuske, K. R., Horvitz, H. R., Bessereau, J. L., Jorgensen, E. M., and Jin, Y. S. (2009) A neuronal acetylcholine receptor regulates the balance of muscle excitation and inhibition in Caenorhabditis elegans. *PLoS Biol.* **7**, e1000265
53. Culetto, E., Baylis, H. A., Richmond, J. E., Jones, A. K., Fleming, J. T., Squire, M. D., Lewis, J. A., and Sattelle, D. B. (2004) The Caenorhabditis elegans unc-63 gene encodes a levamisole-sensitive nicotinic acetylcholine receptor alpha subunit. *J. Biol. Chem.* **279**, 42476–42483
54. Halevi, S., McKay, J., Palfreyman, M., Yassin, L., Eshel, M., Jorgensen, E., and Treinin, M. (2002) The C-elegans ric-3 gene is required for maturation of nicotinic acetylcholine receptors. *EMBO J.* **21**, 1012–1020
55. Hernando, G., Berge, I., Rayes, D., and Bouzat, C. (2012) Contribution of subunits to Caenorhabditis elegans levamisole-sensitive nicotinic receptor function. *Mol. Pharmacol.* **82**, 550–560
56. Lewis, J. A., Wu, C. H., Berg, H., and Levine, J. H. (1980) The genetics of levamisole resistance in the nematode Caenorhabditis-elegans. *Genetics* **95**, 905–928
57. Lewis, J. A., Wu, C. H., Levine, J. H., and Berg, H. (1980) Levamisole-resistant mutants of the nematode Caenorhabditis-elegans appear to lack pharmacological acetylcholine-receptors. *Neuroscience* **5**, 967–989
58. Gottschalk, A., and Schafer, W. R. (2006) Visualization of integral and peripheral cell surface proteins in live Caenorhabditis elegans. *J. Neurosci. Methods* **154**, 68–79
59. Dalliere, N. (2015) *Delineation of a Gut Brain Axis That Regulates Context-Dependent Feeding Behaviour of the Nematode Caenorhabditis elegans*. Doctoral Thesis, University of Southampton
60. Trojanowski, N. F., Padovan-Merhar, O., Raizen, D. M., and Fang-Yen, C. (2014) Neural and genetic degeneracy underlies Caenorhabditis elegans feeding behavior. *J. Neurophysiol.* **112**, 951–961
61. Raizen, D. M., Lee, R. Y. N., and Avery, L. (1995) Interacting genes required for pharyngeal excitation by motor-neuron Mc in Caenorhabditis-elegans. *Genetics* **141**, 1365–1382
62. Almedom, R. B., Liewald, J. F., Hernando, G., Schultheis, C., Rayes, D., Pan, J., Schedletzky, T., Hutter, H., Bouzat, C., and Gottschalk, A. (2009) An ER-resident membrane protein complex regulates nicotinic acetylcholine receptor subunit composition at the synapse. *EMBO J.* **28**, 2636–2649
63. Blanco, M. G., Vela Gurovic, M. S., Silbestri, G. F., Garelli, A., Giunti, S., Rayes, D., and De Rosa, M. J. (2018) Diisopropylphenyl-imidazole (DII): A new compound that exerts anthelmintic activity through novel molecular mechanisms. *PLoS Negl. Trop. Dis.* **12**, e0007021
64. Verma, S., Kashyap, S. S., Robertson, A. P., and Martin, R. J. (2017) Functional genomics in Brugia malayi reveal diverse muscle nAChRs and differences between cholinergic anthelmintics. *Proc. Natl. Acad. Sci. U. S. A.* **114**, 5539–5544
65. Evans, W. J., Morley, J. E., Argiles, J., Bales, C., Baracos, V., Guttridge, D., Jatoi, A., Kalantar-Zadeh, K., Lochs, H., Mantovani, G., Marks, D., Mitch, W. E., Muscaritoli, M., Najand, A., Ponikowski, P., *et al.* (2008) Cachexia: A new definition. *Clin. Nutr.* **27**, 793–799
66. Brenner, S. (1974) The genetics of Caenorhabditis elegans. *Genetics* **77**, 71–94
67. Fay, D. (2006) Genetic mapping and manipulation: Chapter 7-making compound mutants. In: WormBook, ed. *The C. elegans Research Community*, WormBook, Pasadena, CA: 1–4
68. Miyabayashi, T., Palfreyman, M. T., Sluder, A. E., Slack, F., and Sengupta, P. (1999) Expression and function of members of a divergent nuclear receptor family in Caenorhabditis elegans. *Dev. Biol.* **215**, 314–331
69. Mello, C. C., Kramer, J. M., Stinchcomb, D., and Ambros, V. (1991) Efficient gene transfer in C. elegans: Extrachromosomal maintenance and integration of transforming sequences. *EMBO J.* **10**, 3959–3970
70. Kudelska, M. M., Lewis, A., Ng, C. T., Doyle, D. A., Holden-Dye, L., O'Connor, V. M., and Walker, R. J. (2018) Investigation of feeding behaviour in C. elegans reveals distinct pharmacological and antibacterial effects of nicotine. *Invert. Neurosci.* **18**, 14
71. Franks, C. J., Murray, C., Ogden, D., O'Connor, V., and Holden-Dye, L. (2009) A comparison of electrically evoked and channel rhodopsin-evoked postsynaptic potentials in the pharyngeal system of Caenorhabditis elegans. *Invert. Neurosci.* **9**, 43–56
72. Calahorro, F., Keefe, F., Dillon, J., Holden-Dye, L., and O'Connor, V. (2019) Neuroligin tuning of pharyngeal pumping reveals extrapharyngeal modulation of feeding in Caenorhabditis elegans. *J. Exp. Biol.* **222**, jeb189423